Signal optimization design method for integration of communication and radar based on OTFS

Qifeng Meng*, Yan Zhou
School of Information Communication, National University of Defense Technology, Wuhan 410003, Hubei, China

ABSTRACT

Orthogonal Time Frequency Space (OTFS) is an innovative multicarrier modulation method known for its high resilience in challenging Doppler-affected environments, and the integration of communication and radar based on OTFS is expected to be the main development direction of communication and radar integration in unmanned high mobility combat scenarios in the future. In this paper, for the problem that the communication data in the integration of communication and radar based on OTFS would adversely affect the radar ambiguity function, the preprocessing of communication data by using coding sequences with excellent correlation was proposed to improve the effectiveness of the combined signal ambiguity function; furthermore, a Threshold-based Iterative Partial Transfer Sequence method was proposed to reduce the Peak-to-Side Lobes Ratio of the preprocessed integrated signal. The simulation results show that the optimized design scheme of the integrated signal proposed in this paper can improve the distance-dimensional ambiguity function of the integrated signal, and at the same time, the ability of the additive Gaussian White Noise is also significantly enhanced, which can reduce the impact of precoding on Peak-to-Average Power Ratio of the integrated signal, realize highly reliable communication transmission in the case of interference, and achieve excellent radar detection performance.

Keywords: Integration of communication and radar, OTFS, ambiguity function, PAPR

1. INTRODUCTION

Compared with the traditional single radar equipment and communication equipment, the integration of communication and radar has the advantages of multifunctionality, integration, and efficient use of spectrum, which holds significant potential for application in the civil field such as Smart City, intelligent transportation, and the military field, especially in the future intelligent battlefield with high mobility, unmanned, and high confrontation. In the high-mobility battlefield environment, signal design with strong doppler shift and interference resistance, high resolution, and high spectral efficiency is the key to the efficient work of communication and radar integration equipment. Conventional time-frequency domain multicarrier modulation methods, like Orthogonal Frequency Division Multiplexing (OFDM) modulation, which can better counteract the inter-symbol interference performance due to time dispersion in the wireless channel, have been widely used in integrated signals, but the strong doppler in the high mobility scenario, which can destroy the orthogonality between subcarriers of OFDM integrated signals and generate inter-carrier interference, has emerged as a key factor limiting the performance of the current OFDM-based integrated system for further research and development; OTFS is a new multicarrier modulation technique designed specifically for the destructive doppler effect in wireless communication in the delay-doppler domain, so OTFS-based communication and radar integration is expected to become the main development direction of the integration of communication and radar in future unmanned high mobility combat scenarios.

Currently, the research on OTFS mainly focuses on symbol detection, channel estimation, multiple access, etc., and the research on the integration of communication and radar is still in its infancy. Reference[1] applied OTFS technology to the integration communication and radar system and proved that OTFS-based integrated signals has better performance in detection range, tracking rate, and doppler frequency estimation compared with OFDM-based integrated signals. Reference[2] demonstrated that OTFS-based integrated signals provide as accurate distance and velocity estimates as typical radar waveforms and have higher data rates than OFDM-based integrated signals due to fewer cyclic prefixes. In terms of improving the radar ambiguity function, Zhou[3] employed two types of pseudo-random sequences: m-sequence

*mengqifeng612@163.com

International Conference on Optics, Electronics, and Communication Engineering (OECE 2024), edited by Yang Yue, Proc. of SPIE Vol. 13395, 133954J · © 2024 SPIE · 0277-786X · Published under a Creative Commons Attribution CC-BY 3.0 License · doi: 10.1117/12.3049076

and Gold sequence, in the time-frequency domain to pre-code the integrated signal, and demonstrated through simulation that the performance of the integrated signal is improved after coding, the maximum sidelobe value of the distance-dimensional ambiguity function decreases significantly, and the Gold sequence performs better compared to the m sequence; However, only the two common pseudo-random sequences were selected, and there is no study on the Kasami small set[4] and chaotic sequences[5,6], which have better correlation and perform well in OFDM integrated signals, and the effect of precoding on the integrated signals Peak-to-Average Power Ratio (PAPR) is not considered. Because all modulation symbols are uniformly spread in the time-frequency domain, the PAPR of OTFS signals is lower than that of OFDM[7], but similar to OFDM, the OTFS signals still has a high PAPR, two methods were proposed in Reference[8] to reduce the PAPR of OTFS signals, which were Iterative-Partial Transfer Sequence (I-PTS) and Threshold-Selective Mapping (T-SLM), and the effect of these two methods on the system BER, the reduction of PAPR, and the computational complexity were investigated in comparison with μ-law companding technique and Iterative clipping and filtering method, and the simulation results showed that the T-SLM method and the I-PTS method have almost no effect on the BER in terms of the performance of the system BER, whereas the μ-law technique and the Iterative clipping and filtering method cause out-of-band distortion due to the nonlinear transformation of the signals and deteriorate the BER performance, the I-PTS method performs optimally in terms of Peak-to-Average Power Ratio performance, but with higher computational complexity. Reference[9] in the delay-doppler domain also chooses only two types of pseudo-random sequences: the m-sequence and the Gold sequence, to pre-process the communication data and lower the Peak-to-Side Lobes Ratio (PSLR) of the ambiguity function for the combined signals, and then adopts a joint iterative limiting filtering technique to optimize the PAPR of the integrated signals, but fails to optimize the integrated signals for both the time-frequency domain and the delay-doppler domain, the effect of the iterative clipping and filtering method on BER performance has also not been studied.

To this end, based on the studies in References[3,8,9], this paper selects Gold sequence, Kasami small set sequence, and Chebyshev chaotic sequence with excellent correlation characteristics to encode the communication data of the integrated signal beforehand based on OTFS and comparatively analyses the effect on the PAPR of the integrated signals after the precoding of the three sequences. Meanwhile, to address the issue of the high complexity associated with the I-PTS method, the Threshold-based Iterative Partial Transfer Sequence (TS-IPTS) method is proposed, and the simulation results demonstrate that the optimal integrated signal design scheme proposed in this paper achieves both PSLR and PAPR optimization, which can reduce the impact of precoding on the integrated signal PAPR, achieve highly reliable communication transmission under interference conditions, and obtain excellent radar detection performance.

2. OTFS-BASED INTEGRATED SIGNAL MODELLING

In the OTFS-based integrated system, at the transmitter, the transmitted communication data symbols $x_{k,l}$ are treated as grid points in the delayed-doppler domain, $x_{k,l}$ was converted into time-frequency data symbols $X_{n,m}$ using the Inverse Symplectic Finite Fourier Transform (ISFFT), followed by, the baseband signal $s(t)$ is obtained by multicarrier modulation through the Heisenberg transform for transmission. At the receiver, the echo is first demodulated using the Wigner transform and then sampled to obtain delayed-doppler domain data symbols through the Symplectic Finite Fourier Transform (SFFT)[10,11].

The delay-doppler domain data symbols $x_{k,l}$ are transformed to time-frequency domain data symbol $X_{n,m}$ by ISFFT:

$$X_{n,m} = \mathrm{ISFFT}(x_{k,l}) = \frac{1}{\sqrt{NM}} \sum_{l=0}^{M-1} \cdot \sum_{k=0}^{N-1} x_{k,l} e^{j2\pi(\frac{ml}{M} - \frac{nk}{N})} \tag{1}$$

The baseband signal $s(t)$ is derived by applying the Heisenberg transform to equation (1):

$$s(t) = \sum_{m=0}^{M-1} \cdot \sum_{n=0}^{N-1} X_{n,m} g_{tx}(t - mT) e^{j2\pi f_n(t-mT)} \leftarrow \tag{2}$$

where g_{tx} denotes the transmitting rectangular pulse, **M** is the number of symbols, **N** is the number of subcarriers, **T** is the length of a time slot, and f_n is the subcarrier frequency.

3. AMBIGUITY FUNCTION FOR OTFS INTEGRATION SIGNALS

The ambiguity function serves as a valuable mathematical tool for analyzing radar signals and designing waveforms, which is used to describe the radar's resolution, measurement accuracy and other properties, and the radar ambiguity function graph generally has four types: knife-edge, slanting knife-edge, pegboard, and peg, of which the peg-shaped ambiguity function graph with high target detection accuracy and resolution is the target of general radar waveform design. The ambiguity function will no longer change after the radar signal is designed according to the performance requirements, but for the communication and radar integration signal, the ambiguity function changes due to the transmission of communication data over time, which in turn affects the radar detection performance. The ambiguity function for conventional radar signals can be described as:

$$\chi(\tau, f_d) = \int_{-\infty}^{\infty} s(t) s^*(t-\tau) e^{j2\pi f_d t} d_t \tag{3}$$

where $s(t)$ represents the emitted integrated signal, $s^*(t)$ is the conjugate representation of the emitted signal, $\tau = 2R/c$ represents the time delay (where R : the distance between the target and the radar, and c : is the propagation speed of the electromagnetic wave in the air), and $f_d = 2v/\lambda$ is the doppler shift (v : the relative velocity between the target and the radar, λ : the wavelength of the carrier wave).

Substituting the OTFS signal expression into equation (3) yields an expression for the ambiguity function of the integrated signal as:

$$\begin{aligned}
&\chi(\tau, f_d) = \int_{-\infty}^{\infty} s(t) s^*(t-\tau) e^{j2\pi f_d t} dt \\
&= \int_{-\infty}^{\infty} \sum_{m=0}^{M-1} \sum_{n=0}^{N-1} x_{n,m} e^{i2\pi f_n (t-mT)} g_{tx}(t-mT) \\
&\times \sum_{q=0}^{M-1} \sum_{p=0}^{N-1} x_{p,q}^* g_{tx}(t-\tau-qT) e^{-j2\pi f_p (t-\tau-qT)} e^{j2\pi f_d t} dt \\
&= \sum_{m=0}^{M-1} \sum_{n=0}^{N-1} \sum_{q=0}^{M-1} \sum_{p=0}^{N-1} x_{n,m} x_{p,q}^* e^{j2\pi f_p \tau} \\
&\times \int_{T_{min}}^{T_{max}} g_{tx}(t-mT) g_{tx}(t-\tau-qT) e^{j2\pi (f_n + f_d - f_p) t} dt
\end{aligned} \tag{4}$$

$T_{min} = \max(\mathrm{mT}, \mathrm{qT}+\tau)$, $T_{max} = \min((\mathrm{m}+1)\mathrm{T}, (\mathrm{q}+1)\mathrm{T}+\tau)$. According to equation:

$$\int_{T_{min}}^{T_{max}} \mathrm{e}^{-j2\pi t} dt = T_{diff} sinc(\pi f T_{diff}) e^{-2j\pi f T_{avg}} \tag{5}$$

where

$$T_{\mathrm{diff}} = T_{\max} - T_{\min},\ T_{avg} = (T_{max} + T_{min})/2,\ sinc(x) = \frac{\sin x}{x}$$

Equation (5) can be obtained by substituting equation (4):

$$\chi(\tau, f_d) = \sum_{m=0}^{M-1} \sum_{n=0}^{N-1} \sum_{q=0}^{M-1} \sum_{p=0}^{N-1} x_{n,m} x_{p,q}^* e^{j2\pi f_p \tau} T_{diff} \times sinc(\pi(f_p - f_n - f_d) T_{diff}) e^{j2\pi (f_n + f_d - f_p) T_{\mathrm{avg}}} \tag{6}$$

Let $\tau = 0$ in equation (6) to get the integrated signal velocity ambiguity function as:

$$\chi(0, f_d) = \sum_{m=0}^{M-1} \sum_{n=0}^{N-1} \sum_{q=0}^{M-1} \sum_{p=0}^{N-1} x_{n,m} x_{p,q}^* T_{diff} \times sinc\left(\pi(f_p - f_n - f_d) T_{diff}\right) e^{2\pi j (f_n + f_d - f_p) T_{arg}} \tag{7}$$

Let $f_d = 0$ in equation (6) to get the integrated signal distance ambiguity function as:

$$\chi(\tau,0)=\sum_{m=0}^{M-1}\sum_{n=0}^{N-1}\sum_{q=0}^{M-1}\sum_{p=0}^{N-1}x_{n,m}x_{p,q}^{*}e^{j2\pi\left(f_n-f_p\right)T_{avg}}\times T_{diff}\,sinc\left(\pi(f_p-f_n)T_{diff}\right)e^{j2\pi f_p\tau} \tag{8}$$

By examining the ambiguity function equations (7) and (8) of the integrated OTFS signal, it becomes evident that temporal variations in the transmitted communication data $x_{n,m}$ over time will alter the ambiguity function, thereby affecting the radar performance of the integrated communication and radar signal.

4. PSLR-PAPR JOINT OPTIMISED DESIGN SOLUTION

The joint PSLR-PAPR optimal design based on OTFS consists of two main steps: firstly, the coding sequence with excellent correlation characteristics is selected to pre-process the integrated signal in order to reduce its PSLR; and then the TS-IPTS method is applied to reduce the PAPR of the integrated signal. Figure 1 illustrates the flowchart of the joint optimal design scheme.

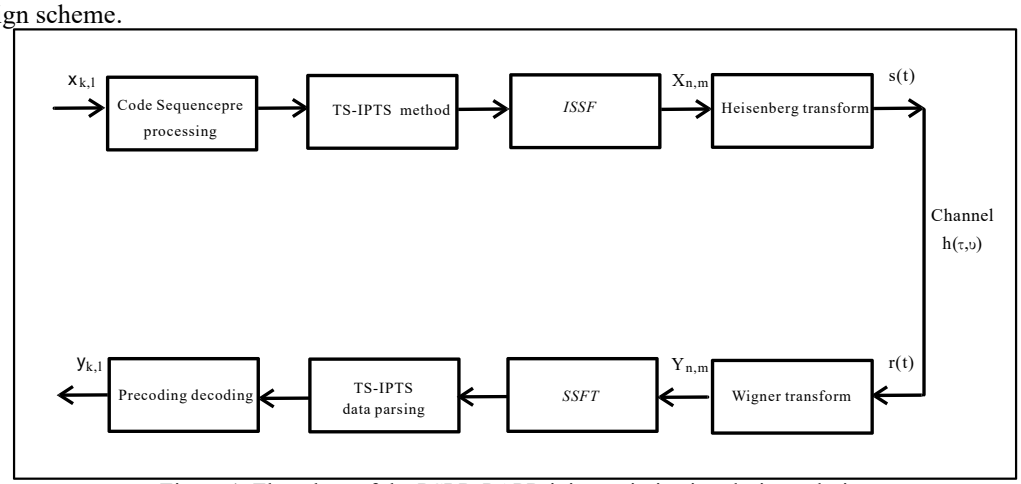

Figure 1. Flowchart of the PSLR-PAPR joint optimization design solution.

4.1 Code sequence

In order to reduce the effect of communication data on the ambiguity function, this paper proposes to pre-code the communication data. In this approach, the selection of the coding sequence is extremely important. Radar detection requires the determination of information such as the characteristics and position of the target. Ideally, the autocorrelation of the radar signal should be similar to the Dirac delta function, with a sharp main peak and no side flaps. This characteristic can make the radar system more accurate positioning targets, accurately identify the target characteristics, and improving the efficiency and accuracy of signal processing, the radar system requires the coding sequence have good autocorrelation. And in the communication system, we need to ensure that the sequence group has low cross-correlation, the cross-correlation value between different code sequences should be as close to zero as possible, which can help reduce multi-access access and anti-interference ability. Therefore, the selection of coding sequences with excellent autocorrelation and cross-correlation is crucial for integrated signal precoding.

Common coding sequences include the m-sequence, the Gold sequence, and Kasami small set, which differ in terms of period and number of sequences, and the detailed data are listed in Table 1, where $\Phi(n)$ represents the Euler number. Although the m-sequence and Gold sequence have good autocorrelation, the cross-correlation lacks, and the length of the n-order the m-sequence and Gold sequence is $2n$-1, which cannot be chosen flexibly and the number is limited. Kasami small set, similar to the Gold sequence, are pseudo-random sequences constructed based on the m-sequence, which not only inherits the good pseudo-randomness of the m-sequence, but also possesses good autocorrelation and cross-correlation. However, as can be seen from Table 1, the number of Kasami small set is small, which limits its application in multi-access communication. In contrast, chaotic sequences are numerous, easy to generate, with flexible sequence lengths and good confidentiality, as well as ideal autocorrelation and cross-correlation, so they can be applied in integrated waveform design. In the chaotic mapping model, the common classical chaotic mapping includes Logistic chaotic mapping, Tent chaotic mapping, and Chebyshev chaotic mapping, etc. By sampling the chaotic mapped signals and quantizing them according to the corresponding quantization rules, we can obtain the chaotic sequences; in this paper, we choose the fourth-order Chebyshev chaotic sequence with low autocorrelation sidelobes and cross-correlation rms values as the object of study[5].

Table 1. Comparison of the properties of four coding sequences.

Code sequences	Sequence cycle	Sequence number
m-sequence	2^n-1	$\Phi(2^n-1)/n$
Gold sequence	2^n-1	2^n+1
Kasami small set	2^n-1	$2^{n/2}$
Chebyshev chaotic sequence	Arbitrary length	Inf

4.2 Fundamentals of the TS-IPTS methodology

At the transmitter side of the OTFS integrated signal, the output signal, which has undergone the Heisenberg transform, is first amplified to obtain a time-domain signal, which is then transmitted to the wireless channel. However, signals with high PAPR may exceed the linear operating range of the amplifier, resulting in signal distortion and aberration. Therefore, an investigation into the Peak-to-Average Power Ratio of the OTFS integrated signal is necessary, and low PAPR signals need to be selected to guarantee that the signal can be within the linear dynamic range of the power amplifier at the transmitter side, to reduce signal distortion and distortion, and to reduce the BER; the Peak-to-Average Power Ratio of the OTFS signal increases linearly with the number of Doppler grids[8]. Preprocessing the code sequence reduces the PSLR of the integrated signal, but it also increases the number of Doppler grids, leading to a rise in the PAPR of the integrated signal. The IPTS method in the literature[8] improves on the traditional PTS and achieves a better compromise between method complexity and performance, but the complexity is still large; the TS-IPTS method is proposed on the basis of the I-PTS method by introducing a reasonable threshold, which significantly reduces the complexity.

The basic principle of the TS-IPTS method is that when adjusting the weighting factors, instead of traversing all possible values, the weighting factors of a sub-block are gradually changed within the range of the set of rotation factors. The adjusted sub-block is compared with the PAPR value of the pre-adjusted sub-block, and the weighting coefficients corresponding to a group of sub-blocks with smaller PAPR values are retained, and in turn, if they are smaller than the pre-set threshold $PAPR_{threshold}$, they are sent directly to the wireless channel; if they are larger, the weighting coefficient value of the sub-block continues to be adjusted, and then the PAPR comparison is performed again. The specific steps of the method are shown in Table 2.

Table 2. A threshold-based iterative partial transfer sequence method.

Steps	Movement
Step 1	For the original communication data $x_{k,l}$ with the number of delay grids **N** and doppler grids **M**, n=0, 1, ..., N-1, m=0, 1, ..., **M**-1, the doppler grids are randomly partitioned into **V** groups, and the delay-doppler signals of each group are $x_{v(k,l)}$, and the number of doppler grids containing the original data is **M/V**, and the number of time-delay grids is N, v=1, 2, ..., **V**.
Step 2	Let the set of rotation factors **b**={1, -1, j, -j}, the index number **index**=1, and the weighting factor of all sub-blocks $b_{v,index}$ =1, v=1, 2, ..., V, to find the Peak-to-Average Power Ratio $PAPR_0$.
Step 3	Compare it with the pre-set threshold $PAPR_{threshold}$ and judge whether it satisfies $PAPR_0 < PAPR_{threshold}$; if it does, it is sent directly to the wireless channel, if it doesn't, then v=v+1, **index**=2.
Step 4	Make weighting factor $b_{v,index} = b(index)$, **index**=**index**+1, judge whether **index**≤length(**b**) is satisfied, if not then v=v+1, index=2, jump back to step 4.
Step 5	Calculate $PAPR$, determine if $PAPR > PAPR_0$ is satisfied, satisfy the condition, and let $b_{index-1} = b(index-1)$; if not, satisfy the condition and let $PAPR_0 = PAPR$.
Step 6	Determine whether v≤**V** is satisfied, jump back to step 4 if it is satisfied, and continue to execute the method if it is not satisfied.

Steps	Movement
Step 7	The final weighting coefficients for all sub-blocks b_v, v=1, 2, ..., **V**, and the required Peak-to-Average Power Ratio is $PAPR_0$.

5. SIMULATION RESULTS AND ANALYSIS

In this paper, we utilize the MATLAB simulation platform to model the OTFS integrated signals, mainly using the Complementary Cumulative Distribution Function (CCDF) of PAPR and PSLR to quantitatively compare and analyze the performance of the ambiguity function and the Peak-to-Average Power Ratio of different integrated signals.

PSLR is defined as the ratio of the maximum sidelobe peak P_S to the main peak P_m, as shown in equation (9).

$$PSLR(dB) = 10lg_{10}^{\frac{P_s}{P_m}} \tag{9}$$

PAPR is defined as the ratio between peak power and average power of the data signal as, as presented in equation (10).

$$\mathrm{PAPR(dB)} = 10lg_{10}^{\frac{\max\limits_{0\leqslant t\leqslant T}|s(t)|^2}{E[|s(t)|^2]}} \tag{10}$$

where $s(t)$ is the time-domain sequence of the data information, $E[.]$ denotes the expectation, the distribution of $PAPR$ is usually represented by the Complementary Cumulative Distribution Function (CCDF), which denotes the probability of $PAPR$ exceeding the threshold $PAPR_0$, as shown in equation (11)[12].

$$CCDF = Pr[PAPR > PAPR_0] \tag{11}$$

5.1 Simulation of PSLR performance for integrated signals based on precoding

The Gold sequence is generated by the preferred pair of the m-sequence with feedback coefficients of 103 and 147, and the coding sequence length is 63; the Kasami small set is obtained by the m-sequence with feedback coefficients of 155 with interval extraction and period extension; and the Chebyshev chaotic sequence has a power series of 4 and an initial value of 0.05. The autocorrelation properties of the three sequences and the cross-correlation properties are shown in Figures 2 and 3.

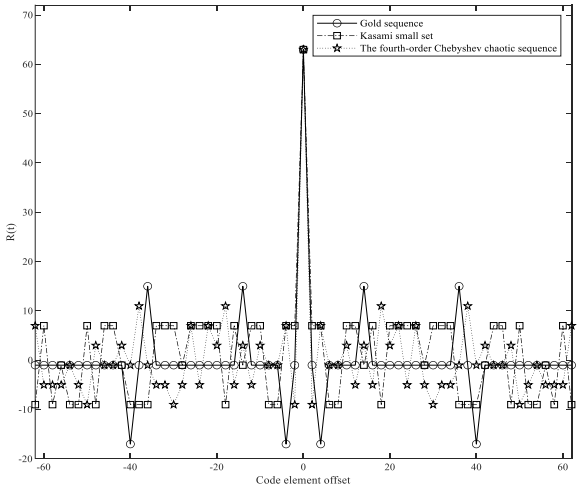

Figure 2. Autocorrelation properties of three coding sequences.

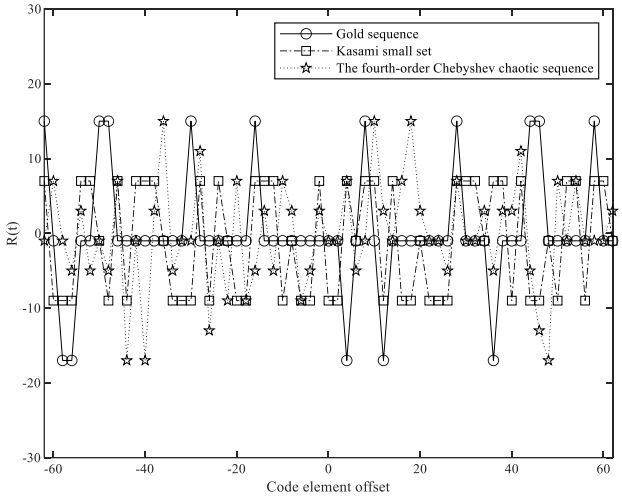

Figure 3. Cross-correlation properties of three coding sequences.

From Figure 2, it can be seen that the Gold sequence has a larger para-valve in the autocorrelation function curve than the fourth-order Chebyshev chaotic sequence and Kasami small set, and the fourth-order Chebyshev chaotic sequence

has a slightly larger para-valve in the autocorrelation curve than the Kasami small set. Therefore, it can be seen that the fourth-order Chebyshev chaotic sequence and Kasami small set are better than the Gold sequence in terms of autocorrelation. According to the data in Figure 3, the curve of the Kasami small set is lower in comparison to the fourth-order Chebyshev chaotic sequence and Gold sequence, so it can be concluded that the Kasami small set has better cross-correlation properties.

In this section, the system parameters have been configured with 6 subcarriers and 4 time slots, a carrier frequency of 1 MHz, the symbol period of 1 us, and 4 PSK modulation. By performing 100 Monte Carlo experiments and calculating the average value, we have analyzed the performance of the ambiguity function. Figures 4 and 5 illustrate the radar ambiguity function for the OTFS integrated signal and the OTFS integrated signal pre-coded with the Kasami small set.

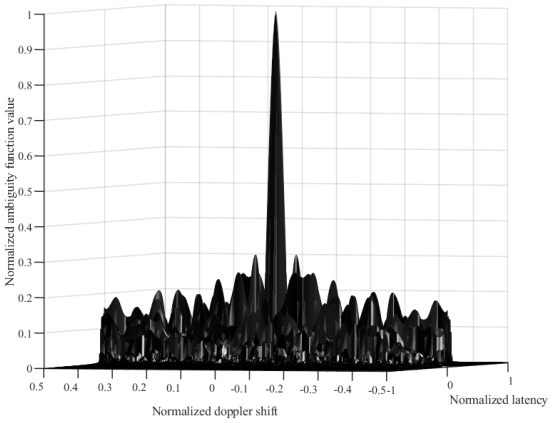

Figure 4. Ambiguity function map for integrated signals based on OTFS

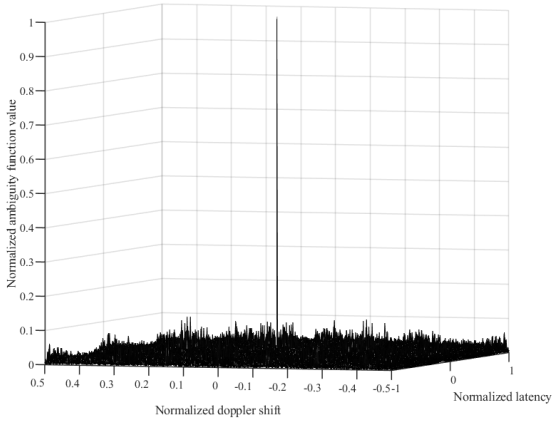

Figure 5. Ambiguity function map of integrated signals based on the Kasami small set-OTFS.

Figure 4 shows that the ambiguity function graph of the original OTFS integrated signal roughly resembles a peg shape, the peak value of the para-flap is high, which affects the accuracy of the target detection, and it can be found by observing the comparison in Figure 5 that the ambiguity function of the OTFS integrated signal pre-coded with the Kasami small set exhibits a sharp peg shape with a narrower main flap, and the para-flap has been significantly suppressed. The para-flap region is flat with lower peaks, which indicates that the OTFS integrated signal pre-coded with the coding sequence with good correlation characteristics has better radar performance.

With the same system parameters and coding sequence length, the communication data are pre-coded with three coding sequences in the delay-doppler domain and time-frequency domain, respectively, and the simulation results are shown in Figures 6 and 7.

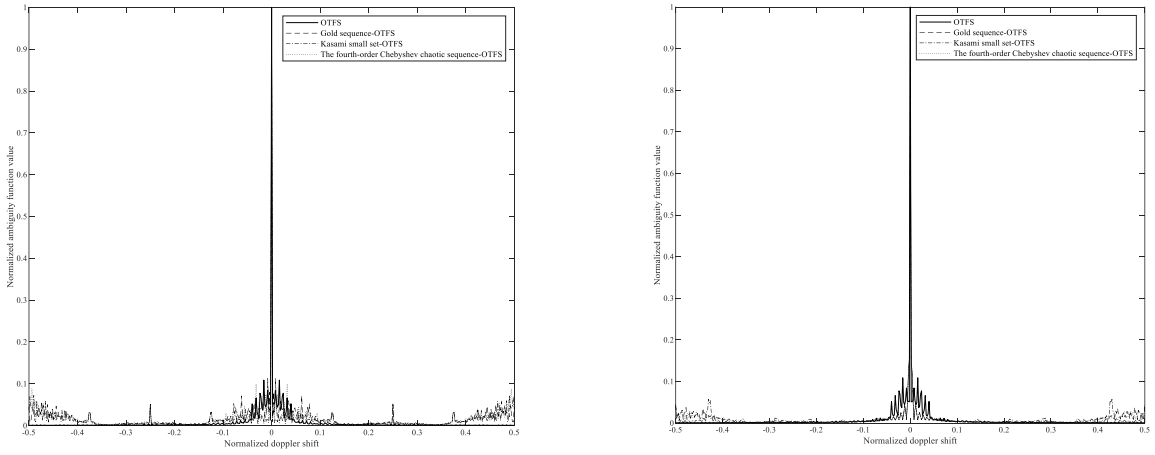

(a). Delay-doppler-domain coding. (b). Time-frequency domain coding.

Figure 6. Velocity-dimensional ambiguity function plots for four integrated signals.

Figure 6 presents the velocity ambiguity functions for the original OTFS integrated signal and the OTFS integrated signal with pre-coding based on the Gold sequence, the Kasami small set, and the fourth-order Chebyshev chaotic sequence. Figures 6a and 6b reveal that the velocity-dimensional ambiguity functions of the OTFS integrated signal and the pre-coded integrated signals are basically the same, which is because the use of coded sequences for the communication data processing doesn't change the duration of the whole data symbols, so the doppler resolution of the integrated signal doesn't change much.

Figure 7 illustrates the distance ambiguity function of the OTFS integrated signal and the OTFS integrated signal pre-coded based on the Gold sequence, the Kasami small set, and the fourth-order Chebyshev chaotic sequence. As can be seen from Figures 7a and 7b, the OTFS integrated signals pre-coded using these three coding sequences have narrower primary flaps and lower sidelobes compared to the original OTFS integrated signals. The simulation results of the four integrated signals in the delay-doppler and time-frequency domains, with different precoding domains, for the distance-dimensional peak para-flap ratio are shown in Table 3. In the table, the distance-dimension PSLR of the original OTFS integrated signal is -6.89 dB, and the pre-coded integrated signals decreases significantly, with -12.19 dB and -9.03 dB for the Gold sequence, -12.21 dB and -8.98 dB for the Kasami small set, and -12.78 dB and -9.05 dB for the fourth-order Chebyshev chaotic sequence. According to the simulation results that the precoding is more effective in the delayed-doppler domain because the ISSF transform is performed after precoding, which enhances the independence of the data symbols, and the integrated signal pre-coded based on the fourth-order Chebyshev chaotic sequence has less fluctuation in the paraboloids region and lower PSLR compared with the Gold sequence and the Kasami small set. The PSLR of the pre-coded OTFS integrated signal is significantly reduced, which indicates that the precoding of the OTFS integrated signals using a coding sequence with excellent correlation characteristics can mitigate the impact of the transmitted communication data on the radar blurring of the integrated signal, thereby enhancing the detection performance of the OTFS integrated signal.

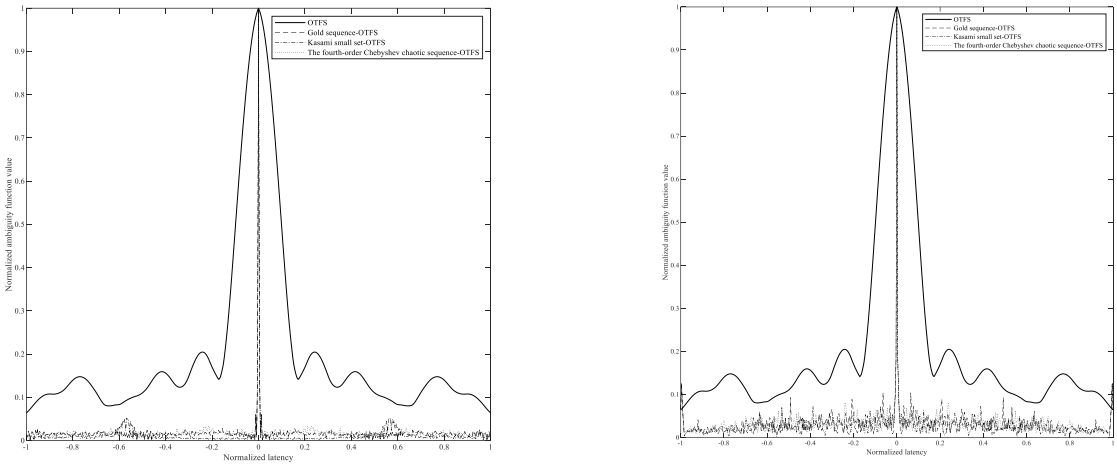

(a). Delay-doppler-domain coding. (b). Time-frequency domain coding.

Figure 7. Distance-dimensional ambiguity function plots for four integrated signals.

Table 3. The Peak-to-Side Lobes Ratio of the integrated signal (in dB).

Integrated signals	Distance dimension ambiguity function PSLR	
	Delay-doppler-domain coding	Time-frequency domain coding
The original OTFS integration signal	-6.89	-6.89
Gold sequence pre-coded OTFS integration signal	-12.19	-9.03
Kasami small set pre-coded OTFS integration signal	-12.21	-8.98
The fourth-order Chebyshev chaotic sequence pre-coded OTFS integration signal	-12.78	-9.05

5.2 TS-IPTS based integrated signal PAPR performance simulation

To assess the effectiveness of the TS-IPTS method in reducing the PAPR of the integrated signals, the system parameters are configured as follows: 6 subcarriers, 8 time slots, the carrier frequency is 1 MHz, the symbol period is 1 us, the 4QAM modulation method is used, the subblocks are randomly segmented, the number of segments is **V**=4, and the threshold is set at 9 dB; The CCDF curves of the original OTFS integrated signal as well as the integrated signal based on the preprocessed Gold sequence, Kasami small set, and the fourth-order Chebyshev chaotic sequence are simulated before and after the suppression of the PAPR by the I-PTS and TS-IPTS methods, and Figure 8 illustrates the results of the simulation.

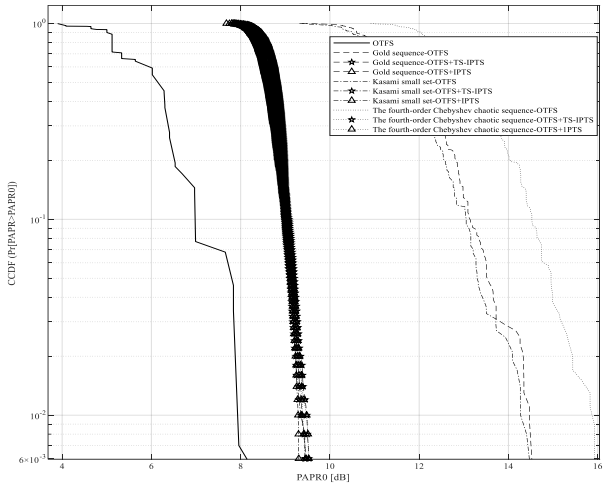

Figure 8. Integrated signal CCDF curve.

As can be seen in Figure 8, at CCDF=6×10^{-3}, the original OTFS integrated signal $PAPR_0$ is 8.17 dB, and the integrated signals based on the preprocessing of the Gold sequence, the Kasami small set, and the fourth-order Chebyshev chaotic sequence are 14.52 dB, 14.47 dB, and 15.94 dB, respectively; there is a significant increase in the PAPR of the integrated signals using the preprocessing, which is due to the increase in the number of doppler grids of the OTFS integrated signals caused by preprocessing. Among them, the Kasami small set only increases by 6.3 dB, which is a better performance, and the fourth-order Chebyshev chaotic sequence is the largest, with an increase of 7.77 dB. At the threshold of 9 dB, the CCDF curves of TS-IPTS and I-PTS after processing are basically coincident, and at CCDF=6×10^{-3}, there are 9.3~9.52 dB, which are slightly larger than the original OTFS integrated signals by 1.13-1.35 dB, and lower than the coded preprocessed integrated signals by 4.95-6.64 dB. After suppression of the integrated signals by the I-PTS method and the TS-IPTS method, the PAPR values of the integrated signals have been suppressed efficiently, and the PAPR values of the integrated signals are different in the two methods. PAPR counts calculated for the integrated signal are shown in Table 4.

Table 4 shows that, regarding computational complexity, the three sequences for which the I-PTS method calculates the PAPR number of times are 273,000 times; the TS-IPTS method under the Gold sequence is 150,296 times; the Kasami small set calculates the number of times the least, at 145,320 times; and the fourth-order Chebyshev chaotic sequence is 154,141 times, compared to the I-PTS method. The computational complexity of the integrated signal, utilizing preprocessing with Gold sequence, Kasami small set, and the fourth-order Chebyshev chaotic sequence, is reduced by nearly 44.9%, 46.8%, and 43.5%, respectively, compared with I-PTS with the same performance, which fully verifies the feasibility and effectiveness of the TS-IPTS method.

Table 4. PAPR counts were calculated for three sequences.

Code sequence	Method	The number of PAPR calculations
Gold sequence	TS-IPTS	150296
	IPTS	273000

Code sequence	Method	The number of PAPR calculations
Kasami small set	TS-IPTS	145320
	IPTS	273000
The fourth-order Chebyshev chaotic sequence	TS-IPTS	154141
	IPTS	273000

5.3 Simulation of integrated signal communication performance with joint optimal design

The main comparison is to analyze the BER of the original OTFS integration signal as well as the integration signals based on the joint optimal design of the Gold sequence, Kasami small set, and the fourth-order Chebyshev chaotic sequence in an additive Gaussian White Noise environment. The simulation conditions remain consistent with those in the previous section, and the signal detection is performed at the receiver side using the message passing method (MP)[13], and the simulation results are shown in Figure 9.

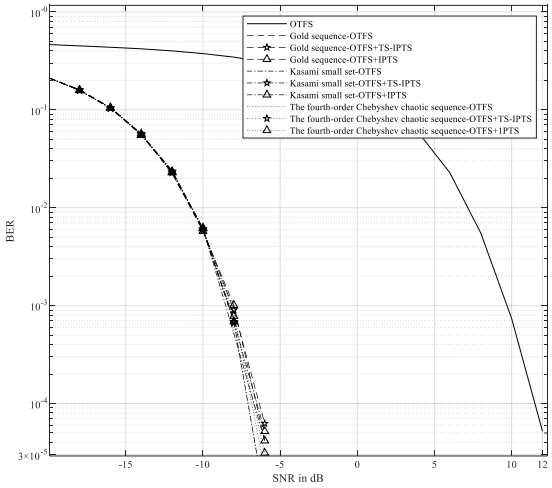

Figure 9. System communication BER chart.

The joint optimization design scheme proposed in this paper uses coding sequences to pre-code the data information on the delay-doppler domain, which can be regarded as a direct expansion operation on the precoding-based OTFS communication and radar integrated signal, resulting in a diversity gain for the integrated signal. In Figure 9, we can see that the BER of the precoding OTFS integrated signals achieve an accuracy of 5.21×10^{-5} when the SNR is about -6 dB in the 4 QAM modulation mode, while to achieve the same BER, the SNR of the OTFS communication and radar integrated signal needs to be about 12 dB. This indicates that the precoding-based OTFS communication and radar integrated signal has stronger resistance to Gaussian White Noise interference and is superior to the original OTFS communication and radar integrated signal. At the same time, it can be seen that the system BER after reducing the Peak-to-Average Power Ratio of the integrated signal by the PTS method and the I-PTS method is basically coincident with the BER curve of the integrated signal after preprocessing, which has no effect on the communication BER of the system.

6. CONCLUSIONS

In order to cope with the problem that the OTFS communication and radar integrated signal is affected by the transmitted communication data and reduces the radar detection performance, this paper proposes a joint optimal design scheme for the OTFS communication and radar integrated signal based on precoding and TS-IPTS to reduce the PAPR by theoretically analyzing the OTFS integrated signal model and its ambiguity function, which selects the Gold sequence, Kasami small set, and the fourth-order Chebyshev chaotic sequence for precoding, and the performance of these three sequences is compared and analyzed, and simulation results indicate that following the precoding of coding sequences, the distance-dimensional ambiguity function PSLR of the integrated signal decreases significantly, which lessens the impact of communication data on the ambiguity function performance of the integrated signal; then the paper simulates

and analyses the effect of pre-coding on the PAPR of integrated signal PAPR, the results indicate that the PAPR of the integrated signal increases to varying extents following the precoding of the three coding sequences, and proposed TS-IPTS method, by choosing a reasonable threshold value, can achieve almost the same effect of reducing the PAPR performance of the integrated signal while significantly reducing the computational complexity by more than 40% compared with the I-PTS method; finally, the paper investigates the effect of the joint optimization scheme of PSLR-PAPR joint optimization scheme on the communication performance, the results show that the optimized integrated signal obtains the diversity gain, and the anti-additive Gaussian White Noise capability achieves exponential enhancement; in terms of the coding sequence selection, more factors need to be taken into account in practical applications to select a suitable sequence to improve the performance of the integrated signal.

REFERENCES

[1] Raviteja, P., Phan, K. T. and Hong, Y., "Orthogonal time frequency space (OTFS) modulation-based radar system," arXiv arXiv:1901.09300, (2019).

[2] Lorenzo, G., Mari, K., Giuseppe, C. and Giulio, C., "On the effectiveness of OTFS for joint radar parameter estimation and communication," Wireless Communications, IEEE Transactions 19(9), 5951-5965 (2020).

[3] Zhou, H., [Research on Signal Design and Physical Layer Encryption Technology of Radar and Communication Integration Based on OTFS], Beijing: Beijing University of Posts and Telecommunications, Master's Thesis, (2021). (in Chinese)

[4] Hou, Y., Zhou, A. and Guo, X., "Design of orthogonal frequency division multiplexing integrated signal for radar and communication based on precoding," Science Technology and Engineering 21(2), 611-615 (2021).

[5] Tian, L., [Radar Communication Integrated Waveform Design Based on Chaotic Direct Sequence Spread Spectrum], Hunan: Hunan University, Master's Thesis, (2019).

[6] Yi, Z., [Design of Radar Communication Integrated Waveform Based on OFDM], Chengdu: University of Electronic Science and Technology of China, Master's Thesis, (2021). (in Chinese)

[7] Khammammetti, V. and Mohammed, S. K., "OTFS-based multiple-access in high doppler and delay spread wireless channels," IEEE Wireless Communications Letters 8(2), 528-531 (2019).

[8] Zhang, L., [Research on the Method of Reducing Peak-to-Average Power Ratio in Orthogonal Time Frequency Space], Guangzhou: Xidian University, Master's Thesis, (2021). (in Chinese)

[9] Shang, X., Zhang, Z. and Wang, X., "A waveform optimization design method for integration of radar and communication based on OTFS," Tactical Missile Technology 5, 31-37 (2022).

[10] Liu, T., [On Pilot Sequence Design and Channel Estimation in OTFS System], Chengdu: Southwest Jiaotong University, Master's Thesis, (2019). (in Chinese)

[11] Li, T., He, R., Ai, B., et al., "OTFS modulation performance in a satellite-to-ground channel at sub-6-GHz and millimeter-wave bands with high mobility," Frontiers of Information Technology & Electronic Engineering, 22(4), 517-526 (2021).

[12] Yuan, J., Li, S., Zhao, F. and Lai, C., "Research progress on the PAPR reduction technology in VLC OFDM systems," Laser Journal 41, 10 (2020).

[13] Ning, X., Qi, J., Wang, Z. and Zhang, B., "A message passing algorithm with variable damping factor for OTFS," IEEE Wireless Communications Letters 12(11), 1 (2023).